

## DIRECT INFRARED OBSERVATIONS OF THE VERY LOW MASS OBJECT GLIESE 623B

D. W. MCCARTHY, JR.<sup>1</sup> AND T. J. HENRY

Steward Observatory, University of Arizona

Received 1987 April 14; accepted 1987 May 27

### ABSTRACT

A low-mass, probably stellar, companion to the nearby star Gliese 623 has been detected interferometrically at 1.25, 1.65, and 2.2  $\mu\text{m}$ , and its motion has been monitored over more than one full revolution cycle. Detection of this companion confirms a low-amplitude perturbation of the photocenter indicated previously by extensive astrometric observations. The interferometry, together with available astrometric and radial velocity measurements, yields improved orbital elements and the first photometric measurements and mass determinations of the component stars. The indicated luminosity ( $M_{\text{bol}} = 12.3$ ) and mass ( $\sim 0.09 M_{\odot}$ ) of Gl 623B appear inconsistent with stellar models which predict a rapid decline of luminosity with decreasing mass ( $\leq 0.2 M_{\odot}$ ) for stars of age  $\geq 2$  Gyr.

*Subject headings:* infrared: sources — interferometry — stars: binaries — stars: evolution — stars: late-type

### I. INTRODUCTION

Gliese 623 (CC 20,986;  $m_V = 10.3$ ; M3 V) is a high proper-motion star and astrometric binary at a distance of 7.5 pc. Long-focus photographic astrometry has revealed a weak ( $0''.08$  peak) perturbation of the photocenter suggestive of a companion star near the mass limit of the hydrogen-burning main sequence (Lippincott and Borgman 1978). A low-mass companion has been confirmed by direct detection of its infrared emission at 2.2  $\mu\text{m}$  (McCarthy 1983, 1986) and by accurate measurement of radial velocities (Marcy *et al.* 1986). However, Marcy *et al.* suggest the possibility of two companions in order to explain differences in the orbital period derived from the astrometric and velocity measurements.

In this *Letter*, we combine new infrared measurements of the relative orbit and apparent magnitudes with existing astrometric and radial velocity data to derive the masses and absolute magnitudes of the components and to improve the orbital elements. A binary system is consistent with all available data. The photocentric orbit of Gl 623 is the lowest amplitude astrometric perturbation yet confirmed directly. These results demonstrate the effectiveness of combining data obtained by independent techniques in order to study low-mass stars and to calibrate the lower main sequence.

### II. OBSERVATIONS

Gl 623 has been directly resolved by the technique of one-dimensional infrared speckle interferometry in the standard photometric bands at  $J$  (1.25  $\mu\text{m}$ ),  $H$  (1.65  $\mu\text{m}$ ), and  $K$  (2.2  $\mu\text{m}$ ). Details of this technique and the current observing procedures are described by McCarthy (1986). Observations were obtained over more than one revolution cycle between

epochs 1982.35 and 1987.19, using the Steward Observatory 2.24 m and Kitt Peak 3.8 m telescopes. One-dimensional scans of the instantaneous image were obtained at rates between 50 and 100 arcsec  $\text{s}^{-1}$ . Calibration of the speckle transfer function was accomplished frequently by alternating observations of Gl 623 and an unresolved star, SAO 46128. The differential air mass between these two sources was negligible.

Table 1 summarizes interferometric measurements of angular separations, brightness ratios, and apparent magnitudes at the different epochs and position angles. These parameters have been derived from least-squares fits to a binary model using only the visibility amplitudes. The damping effect discussed by McCarthy, Cobb, and Probst (1987) is negligible at these spatial frequencies for the indicated brightness ratio.

Figure 1 illustrates typical visibility amplitudes and phases as measured with the 3.8 m telescope at a  $45^\circ$  position angle at epoch 1986.46 (JD 2,446,598). Phases were calculated using the Knox-Thompson algorithm (Knox and Thompson 1974). The binary nature of Gl 623 is clearly indicated with an angular separation of  $0''.33$  and a brightness difference of 2.81 mag at 2.2  $\mu\text{m}$ . These spatial frequency measurements can be Fourier transformed to reconstruct an image (see McCarthy, Cobb, and Probst 1987). Errors in spatial calibration yield a typical uncertainty of  $\pm 5\%$  in angular separation.

### III. INTERFEROMETRIC RESULTS

#### a) Photometry

Photometry from 11 nights of speckle interferometry yields an apparent magnitude for the Gl 623 system of  $5.77 \pm 0.04$  mag at 2.2  $\mu\text{m}$ . This magnitude compares favorably with the value of  $5.91 \pm 0.02$  measured by Stauffer and Hartmann (1986). From the mean brightness ratio at 2.2  $\mu\text{m}$  ( $2.91 \pm 0.15$  mag) and the known absolute parallax ( $\pi = 0''.134$ , standard error =  $\pm 0.0074$ ; Lippincott and Borgman 1978), we derive

<sup>1</sup>Visiting Astronomer, Kitt Peak National Observatory, National Optical Astronomy Observatories, operated by the Association of Universities for Research in Astronomy, Inc., under contract with the National Science Foundation.

TABLE 1  
 INFRARED SPECKLE MEASUREMENTS

| Julian Day<br>(2,440,000 +) | Position<br>Angle | Separation | Brightness<br>Ratio<br>(mag) | $m_K$       | Scale Factor<br>$(B - \beta)^{-1}$ |
|-----------------------------|-------------------|------------|------------------------------|-------------|------------------------------------|
| 5095                        | 0°                | 0".28      | 3.04                         | ...         | 5.83 <sup>a</sup>                  |
| 5158                        | 90                | 0.25       | ...                          | ...         | 6.45 <sup>a</sup>                  |
| 5774                        | 0                 | ...        | ...                          | ...         | ...                                |
| 5775                        | 90                | ≤ 0.05     | ...                          | 5.81        | ...                                |
| 5800                        | 90                | ...        | ...                          | 5.77        | ...                                |
| 5801                        | 90                | ...        | ...                          | 5.78        | ...                                |
| 6185                        | 0                 | 0.12       | ...                          | 5.72        | 7.19                               |
| 6216                        | 0                 | 0.14       | ...                          | 5.72        | 6.73                               |
| 6454                        | 90                | ...        | ...                          | 5.86        | ...                                |
| 6538                        | 90                | 0.23       | ...                          | 5.72        | 6.27                               |
| 6539                        | 0                 | 0.28       | 2.85                         | 5.80        | 5.19 <sup>a</sup>                  |
|                             | 45                | 0.39       | 3.10                         | 5.74        | 6.08 <sup>a</sup>                  |
| 6598                        | 45                | 0.33       | 2.81                         | 5.75        | 5.41 <sup>a</sup>                  |
|                             | 135               | 0.10       | ...                          | ...         | 5.10                               |
| 6805                        | 0                 | 0.35       | 2.76                         | ...         | 6.55 <sup>a</sup>                  |
| 6806                        | 90                | ≤ 0.12     | ...                          | ...         | ...                                |
| 6867                        | 90                | ≤ 0.05     | ...                          | 5.77        | ...                                |
| 6868                        | 0                 | 0.26       | 3.00 <sup>b</sup>            | ...         | 5.52 <sup>a</sup>                  |
|                             | 0                 | ...        | 3.28 <sup>c</sup>            | ...         | ...                                |
| Averages                    |                   |            | 2.91 ± 0.15                  | 5.77 ± 0.04 | 5.86 ± 0.52                        |

<sup>a</sup>Indicates fully resolved ( $\geq 0''.25$ ) separation component used in determining scale factor.

<sup>b</sup>Indicates measurement at  $H$  ( $1.65 \mu\text{m}$ ).

<sup>c</sup>Indicates measurement at  $J$  ( $1.25 \mu\text{m}$ ).

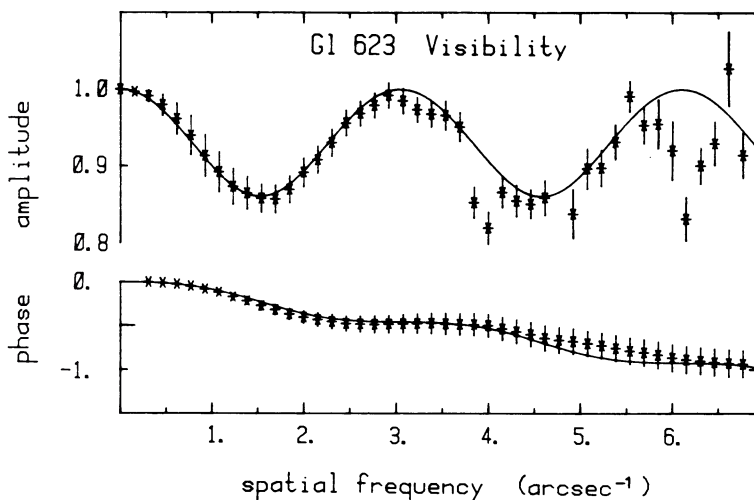


FIG. 1.—Measurements of visibility amplitude and phase (radians) vs. spatial frequency at  $2.2 \mu\text{m}$ , obtained at epoch 1986.46 with the 3.8 m telescope at a  $45^\circ$  position angle. Solid lines are based on a binary model fitted to the amplitude data. The companion lies to the northeast with an angular separation of  $0''.33$  and a brightness ratio of 2.81 mag.

individual absolute magnitudes ( $M_K$ ) for the component stars of 6.5 and 9.4. From empirical main-sequence relationships (Veeder 1974; Berriman and Reid 1987), the corresponding bolometric magnitudes are 9.1 and 12.3, yielding mass estimates of 0.34 and  $0.084 M_\odot$ , respectively.

From the measured brightness ratios at  $J$  and  $H$  and the absolute photometry from Stauffer and Hartmann (1986), we derive  $(J - H, H - K)$  colors of (0.51, 0.34) and (0.79, 0.44) for the primary and secondary components, respectively. Thus,

in the two-color diagram, the primary is located in a region populated by metal-poor stars. The secondary is redder with colors nearly identical to those of the brown dwarf candidate LHS 2924 (Probst and Liebert 1983) and the low luminosity objects RG 0050.5-2722 and VB 10 (Reid and Gilmore 1981).

The expected magnitude difference in the  $V$  band is 5.2 mag. Consequently, the fractional luminosity  $\beta$  of the secondary is negligible (Feierman 1971), and the photocentric orbit is also the orbit of the primary star.

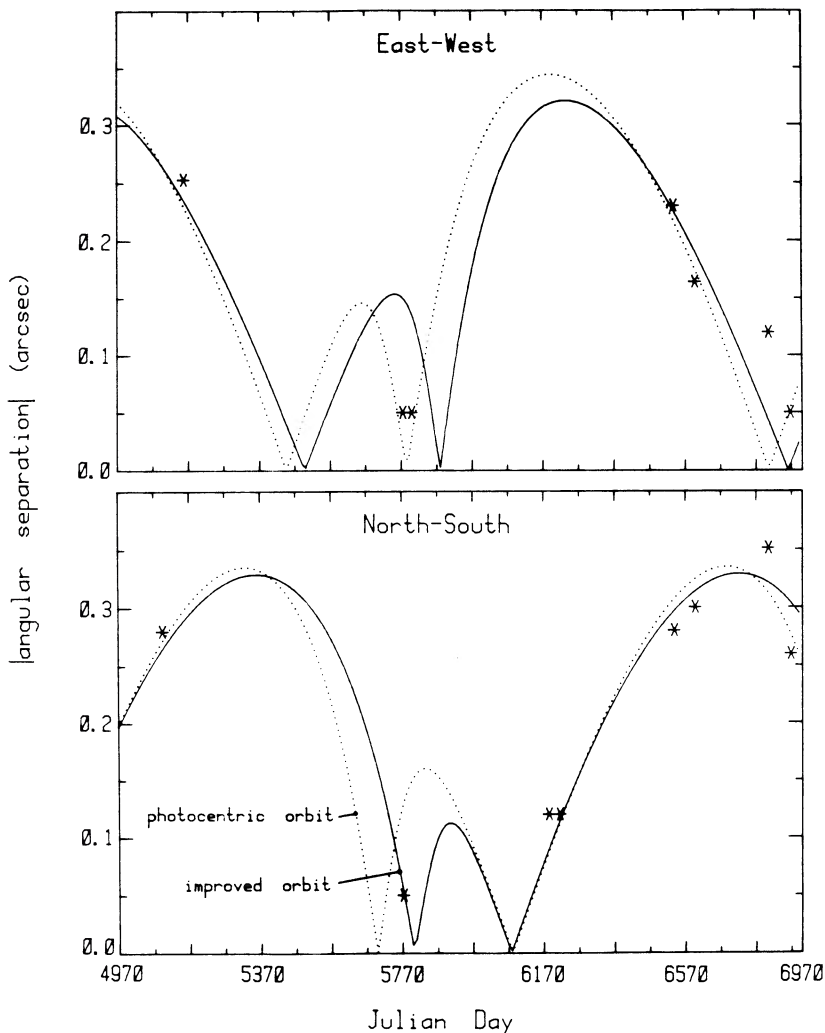


FIG. 2.—Absolute values of angular separations measured from  $2.2 \mu\text{m}$  speckle interferometry vs. Julian day for north-south and east-west position angles. Measurements at other position angles have been projected accordingly. Dotted lines illustrate angular separations expected from the photocentric orbital elements and the scale factor, 5.86, indicated by the speckle work alone. Solid lines indicate separations expected from the improved orbital elements and new scale factor, 5.61.

#### b) The Relative Orbit

Table 1 also summarizes the calculated scale factor,  $(B - \beta)^{-1} = B^{-1}$  between the photocentric and relative orbits, where  $B$ , the fractional mass, equals  $M_B(M_A + M_B)^{-1}$ . At a given epoch and position angle, this scale factor equals the ratio of the measured separation to the predicted position of the photocenter as calculated from the photocentric orbital elements (Lippincott and Borgman 1978). Including only measurements which fully resolve the separation (i.e.,  $\geq 0''.25$ ) and therefore allow the brightness ratio to be determined unambiguously, we find  $B^{-1} = 5.86 \pm 0.52$ .

The infrared separation measurements provide one check on the accuracy of the photocentric orbital elements. Figure 2 illustrates the generally excellent agreement between these measurements and the photocentric orbit scaled by the above factor. However, because of the orientation of the true orbit (see Table 2), the apparent orbit has lower eccentricity,  $\sim 0.2$ ,

so the speckle measurements do not provide a sensitive check on these elements.

#### IV. IMPROVEMENT OF THE ORBITAL ELEMENTS

A second check on the photocentric orbital elements is provided by recent radial velocity measurements of the primary star (Marcy *et al.* 1986). Figure 3 shows these measurements as well as the velocity curve predicted from the photocentric orbital elements and parallax. Although the amplitudes are equal to within 10%, the agreement between these curves is not good. This comparison suggests that the elements can be improved, particularly the time of periastron passage,  $T_0$ , and/or the period,  $P$ , which together determine the epoch of rapid velocity change. In addition,  $\omega$ , the longitude of periastron, must lie in the third quadrant (Heintz 1978, p. 82) to explain the direction of velocity change.

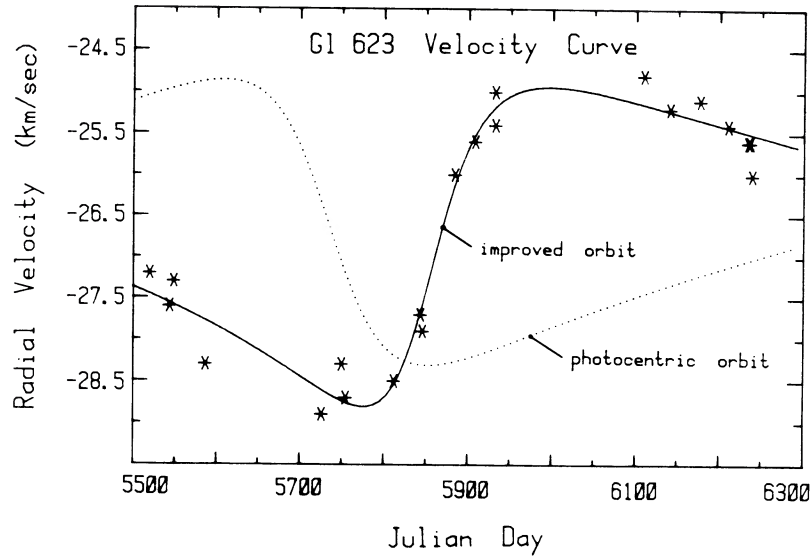


FIG. 3.—Orbital analysis of the radial velocity measurements of G1 623 obtained by Marcy *et al.* (1986), shown as asterisks. Dotted line represents predictions from the photocentric orbital elements using the scale factor, 5.86, derived solely from the infrared speckle measurements. Solid line illustrates predictions from the improved orbital elements and scale factor, 5.61, using the calculated center-of-mass velocity.

In order to improve the orbital elements, we utilized a least-squares procedure which sequentially varies the value of each element to minimize the  $\chi^2$  differences between the photocentric orbital ephemeris and the measurements of both angular separation and radial velocity. This procedure involves a total of eight variable parameters: Six orbital elements ( $P$ ,  $T_0$ ,  $e$ ,  $i$ ,  $\omega$ ,  $\Omega$ ), the velocity of the center of mass, and the scale factor between the true ( $a$ ) and photocentric ( $\alpha$ ) semimajor axes. A fixed parallax,  $0''.134$ , has been assumed. The longitude of the line of nodes,  $\Omega$ , can only be determined from the measurements of angular separation. Since this method is simplistic and involves eight parameters, the resulting solution may not be unique. However, a solution is found which significantly improves the agreement with the radial velocity data as shown in Figure 3. Figure 2 compares the predicted and measured angular separations.

Table 2 summarizes the improved orbital elements. Clearly, they are very similar to the original photocentric elements with the major exceptions of  $T_0$  and  $\omega$ . The new values are also in good agreement with those derived from more recent radial velocity measurements (Marcy 1987). The scale factor is now determined more accurately

$$(B - \beta)^{-1} = B^{-1} = a/\alpha = 5.61 \pm 0.14.$$

These orbital elements appear well determined, are in excellent agreement with three independent data sets (astrometry, infrared speckle, and radial velocity), and are consistent with a binary, rather than a multiple, system. Additional checks of these parameters will come from more extensive speckle and radial velocity measurements. It is important that the latter data sample in more detail the peak of the velocity curve.

TABLE 2  
ORBITAL ELEMENTS AND CENTER-OF-MASS VELOCITY<sup>a</sup>

| Parameter                                       | (Speckle Plus)        |                  |
|---|-----------------------|------------------|
|   | Photocentric          | Radial Velocity) |
| $\alpha$ .....                                  | $0''.049 \pm 0''.003$ | ...              |
| $a$ .....                                       | ...                   | $0''.275$        |
| $P$ (yr) .....                                  | 3.72                  | 3.733            |
| $e$ .....                                       | 0.53                  | 0.58             |
| $T_0$ .....                                     | 1965.50               | 1965.75          |
| $i$ .....                                       | $150^\circ$           | $147^\circ.4$    |
| $\omega$ .....                                  | $93^\circ$            | $254^\circ.7$    |
| $\Omega$ .....                                  | $142^\circ$           | $109^\circ.3$    |
| $V_{\text{system}}$ (km s <sup>-1</sup> ) ..... | ...                   | -26.54           |

<sup>a</sup> Parallax =  $0''.134$ .

## V. DISCUSSION

### a) Mass Measurements

From the parallax, improved orbital elements, and scale factor, we derive the individual masses of the component stars. By Kepler's Third Law, the total mass of the system is  $0.62 \pm 0.16 M_\odot$ . Since the fractional mass  $B$  equals 0.178, the individual masses are  $0.51 \pm 0.16$  and  $0.11 \pm 0.029 M_\odot$ . Errors in  $\alpha$  and  $\pi$  contribute almost equally to errors in these masses. Uncertainty in the scale factor yields mass errors considerably smaller—0.05 and  $0.009 M_\odot$ , respectively. Thus, the mass ratio is relatively well determined.

These masses are both systematically larger than those (0.34, 0.084) estimated from the absolute photometry. For stellar masses  $\geq 0.3 M_\odot$ , the mass-luminosity relation is believed to be well understood (Liebert and Probst 1987).

TABLE 3  
DERIVED MASSES VERSUS PARALLAX

| PARALLAX             | ASTROMETRY PLUS SPECKLE |                        | PHOTOMETRIC            |                        |
|----------------------|-------------------------|------------------------|------------------------|------------------------|
|                      | $M_A$<br>( $M_\odot$ )  | $M_B$<br>( $M_\odot$ ) | $M_A$<br>( $M_\odot$ ) | $M_B$<br>( $M_\odot$ ) |
| 0''110.....          | 0.77                    | 0.18                   | 0.41                   | 0.10                   |
| 0.120.....           | 0.64                    | 0.14                   | 0.38                   | 0.095                  |
| 0.134 $\pm$ 0.0074.. | 0.51                    | 0.11                   | 0.34                   | 0.085                  |
| 0.140.....           | 0.48                    | 0.10                   | 0.32                   | 0.081                  |
| 0.150.....           | 0.43                    | 0.088                  | 0.30                   | 0.075                  |
| 0.160.....           | 0.40                    | 0.078                  | 0.28                   | 0.071                  |

However, the primary mass determined here is too large for the observed spectral type and near-infrared colors and requires a large underluminosity,  $\Delta M_{\text{bol}} = 1.4$  mag. The amount of this discrepancy cannot be explained by errors in Veeder's (1974) empirical main-sequence relationships ( $\Delta M_{\text{bol}} \approx 0.2$ – $0.3$  mag) or by the apparent intrinsic dispersion in  $M_{\text{bol}}$  ( $\sim 0.5$  mag) for a given  $V - K$  color. Furthermore, it cannot be caused by differences in metal abundance (VandenBerg *et al.* 1983). If the primary mass equals  $0.34 M_\odot$ , as indicated by the absolute photometry, then the mass ratio yields a secondary mass of  $0.074 M_\odot$ .

It is possible that the calculated masses are overestimated due to inaccuracy in the parallax. In fact, a significant error in parallax is indicated not only by the standard error,  $\sigma$ , of 5.5% but also by an unusually large discrepancy,  $0''.035 = 4.7 \sigma$ , between the parallaxes measured in right ascension and declination at both the Sproul and Van Vleck observatories (Lippincott and Borgman 1978). To illustrate the dependence of the individual masses on parallax, Table 3 compares, for different values of the parallax, the photometric masses with those masses calculated using the improved orbital elements (after recalculation for each new parallax) and the measured angular separations. At a parallax of  $0''.150$ , the photometric and calculated masses of the primary star are consistent within the uncertainties of the photometric relationships. Since the two methods should give similar results for the primary star, we suspect that the calculated masses are too large because of uncertainty in the parallax. If this assessment is correct, then the mass of the secondary is probably close to, and possibly less than,  $\sim 0.09 M_\odot$ .

#### b) Comparison with Evolutionary Models of Low-Mass Stars

For stellar masses  $\leq 0.2 M_\odot$ , theoretical mass-luminosity relationships (Grossman, Hayes, and Graboske 1974; VandenBerg *et al.* 1983; D'Antona and Mazzitelli 1985) predict a decrease of luminosity with increasing age. The amount of this decrease increases with declining mass. This effect allows a declining luminosity function to translate into a rising initial mass function at low stellar masses (Liebert and Probst 1987) and may thus permit a substantial population of low-mass stars and substellar objects. Gl 623B provides an opportunity to test these expectations since it has low mass ( $0.074$ – $0.11 M_\odot$ ), low luminosity, and, as we next demonstrate, characteristics of old age.

Evidence for an age from 1.5 to  $\geq 5$  Gyr comes from two lines of evidence. First, Gl 623 has old disk space motions. From the radial velocity of its center of mass and the available proper motions and parallax, its space motion is  $64 \text{ km s}^{-1}$  ( $U = 33$ ,  $V = -13$ ,  $W = 53$ ) after correction for standard solar motion ( $U_0 = -10.4$ ,  $V_0 = 14.8$ ,  $W_0 = 7.3$ ; Mihalas and Binney 1981). Wielen (1974) has examined the relation between kinematics and ages of stars in the Gliese catalog by correlating velocity dispersions with ages for stars of spectral types A through G, as well as for McCormick K and M dwarfs. The space velocity of Gl 623 exceeds the  $50 \text{ km s}^{-1}$  velocity dispersion of the K and M dwarfs; therefore, the age of Gl 623 is likely to be greater than the average age of that group, i.e.,  $\geq 5$  Gyr. In addition, an absolute age of  $6.6 \pm 1.7$  Gyr is indicated by the stellar velocity diffusion coefficient method (Wielen 1977).

The Gl 623 system also has photometric and spectroscopic properties characteristic of the oldest, and presumably least chromospherically active, M dwarfs (Stauffer and Hartmann 1986). The primary is significantly metal-poor from its location in the infrared ( $J - H$ ,  $H - K$ ) diagram. Furthermore, Gl 623 has only a weak  $H\alpha$  absorption equivalent width, a characteristic of older stars. Stauffer and Hartmann (1986) discuss the evolution of  $H\alpha$  activity for M dwarfs. From their analysis, approximately one in seven M dwarfs similar to Gl 623 in  $R - I$  exhibits  $H\alpha$  in emission, indicating a minimum age of 1.5 Gyr, assuming constant star formation over the last  $10^{10}$  yr.

D'Antona and Mazzitelli's (1985) models of low-mass stars allow an estimate of the secondary's mass given its luminosity,  $M_{\text{bol}} = 12.3$ , and age, 1.5 to  $\geq 5$  Gyr. These properties indicate a *minimum* mass of  $0.10 M_\odot$ . Thus, the secondary mass,  $0.11 M_\odot$ , calculated from the astrometric and speckle measurements agrees well with the evolutionary models. However, as noted earlier, the resulting primary mass,  $0.51 M_\odot$ , requires a considerable underluminosity relative to normal M dwarfs. A somewhat larger parallax,  $\sim 0''.150$ , is possible and can resolve this discrepancy yielding primary and secondary masses of  $0.43 M_\odot$  and  $0.088 M_\odot$ , respectively. In this case, Gl 623B is  $\sim 1.5$  mag more luminous for its age than predicted by the models. More accurate masses, derived from improved observations, are necessary to resolve the apparent disagreement with evolutionary models of low-mass stars.

#### VI. CONCLUSIONS

We have detected the direct thermal emission from a low-mass astrometric companion to the nearby star Gl 623 and have monitored its relative motion over more than a full revolution period. Speckle interferometry, together with astrometric and radial velocity measurements, yields improved orbital elements that permit determination of the masses. Current measurements yield a secondary mass between  $0.074$  and  $0.11 M_\odot$  with a preferred value near  $0.09 M_\odot$ . This companion is one of the least massive stars known and, because of its probable old age, makes possible a test of recent evolutionary models of low-mass stars. This work suggests that these models may require revision.

The authors acknowledge helpful discussions with Drs. G. Marcy, E. Roemer, R. G. Probst, and J. Liebert. Drs. G. and M. Rieke provided the liquid helium cooled InSb detector

used at the 2.24 m telescope. This work has been supported by the National Science Foundation through grants AST-8218782 and AST-8519506.

## REFERENCES

- Berriman, G., and Reid, N. 1987, *M.N.R.A.S.*, in press.  
 D'Antona, F., and Mazzitelli, I. 1985, *Ap. J.*, **296**, 502.  
 Feierman, B. 1971, *A.J.*, **76**, 73.  
 Grossman, A. S., Hays, D., and Graboske, H. C. 1974, *Astr. Ap.*, **30**, 95.  
 Heintz, W. D. 1978, *Double Stars* (Dordrecht: Reidel).  
 Knox, K. T., and Thompson, B. J. 1974, *Ap. J. (Letters)*, **193**, L45.  
 Liebert, J., and Probst, R. G. 1987, in *Ann. Rev. Astr. Ap.*, in press.  
 Lippincott, S. L., and Borgman, E. R. 1978, *Pub. A.S.P.*, **90**, 226.  
 Marcy, G. W. 1987, private communication.  
 Marcy, G. W., Lindsay, V., Bergengren, J., and Moore, D. 1986, in *Astrophysics of Brown Dwarfs*, ed. M. C. Kafatos, R. S. Harrington, and S. P. Maran (Cambridge: Cambridge University Press), p. 50.  
 McCarthy, D. W. 1983, in *IAU Colloquium 76, The Nearby Stars and the Stellar Luminosity Function*, ed. A. G. D. Philip and A. R. Upgren (Schenectady, NY: Davis), p. 107.  
 ———. 1986, in *Astrophysics of Brown Dwarfs*, ed. M. C. Kafatos, R. S. Harrington, and S. P. Maran (Cambridge: Cambridge University Press), p. 9.  
 McCarthy, D. W., Cobb, M. L., and Probst, R. G. 1987, *A.J.*, in press.  
 Mihalas, D., and Binney, J. 1981, *Galactic Astronomy Structure and Kinematics* (San Francisco: Freeman), p. 398.  
 Probst, R. G., and Liebert, J. 1983, *Ap. J.*, **274**, 245.  
 Reid, I. N., and Gilmore, G. 1981, *M.N.R.A.S.*, **196**, 15P.  
 Stauffer, J. R., and Hartmann, L. W. 1986, *Ap. J. Suppl.*, **61**, 531.  
 VandenBerg, D. A., Hartwick, F. D. A., Dawson, P., and Alexander, D. R. 1983, *Ap. J.*, **266**, 747.  
 Veeder, G. J. 1974, *A.J.*, **79**, 1056.  
 Wielen, R. 1974, in *Highlights Astr.*, **3**, 395.  
 ———. 1977, *Astr. Ap.*, **60**, 263.

T. J. HENRY and D. W. MCCARTHY, JR.: Steward Observatory, The University of Arizona, Tucson, AZ 85721